



*medical imaging,
MRI, brain perfusion*

Bartosz KARCZEWSKI¹, Jacek RUMIŃSKI¹

VALIDITY OF MRI BRAIN PERFUSION IMAGING METHOD

Brain perfusion imaging with Dynamic Susceptibility Contrast MRI is very promising method since it can be easily implemented as a standard contrast-based MRI procedure. We present the results of a set of analysis to validate the DSC-MRI method. The influence of bolus dispersion, delay, low SNR and other possible sources that can influence the final perfusion parameter values were verified. Different methods of perfusion parameters calculations are also presented and compared to discuss the role of a chosen method in quality of brain perfusion images.

1. INTRODUCTION

Parametric images represents values of reconstructed parameters for assumed tissue/activity model. This includes DSC-MRI [3], ASL MRI [5], dynamic PET/SPECT [1], dynamic active thermography [4], etc. In DSC-MRI imaging, after injection of a bolus of contrast agent (e.g. Gd-DTPA), a series of images are measured. This image-sequence data presents local voxel activity of contrast (blood) flow and distribution. It is assumed, that measured MRI signal values are proportional to the contrast concentration. Contrast concentration as a function of time is measured for brain supported arteries which is estimated as the arterial input function (AIF). In real conditions the AIF is not an ideal impulse function (dispersion and delay), additionally in DSC-MRI measurements are done from a volume of interest (VOI) therefore deconvolution is required to calculate VOI impulse response $F^*R(t)$:

$$C_t(t) = \frac{\rho}{Kh} \int_0^t C_a(\tau) \cdot (F \cdot R(t-\tau)) d\tau, \quad (1)$$

where: $C_a(t)$ - contrast concentration in the artery (e.g., Middle Cerebral Artery) – Arterial Input Function AIF, $C_t(t)$ - contrast concentration in the tissue, $\frac{\rho}{Kh}$ - scaling factor (quantitative description), $F^*R(t)$ – scaled impulse response (residue function) inside VOI. The $R(t)$ - represents fractional tissue concentration.

Assuming that contrast material remains intravascular and the first pass of the contrast bolus can be eliminated from the concentration function a set of perfusion related parameters can be calculated (using deconvolution to find $R(t)$). Since $R(t=0)$ should be equal to 1, then

¹ Department of Biomedical Engineering, Gdansk University of Technology,

$$F \cdot R(t=0) = F = rCBF \text{ (regional Cerebral Blood Flow)}. \quad (2)$$

Regional cerebral blood volume (proportional to the normalized total amount of tracer) and mean transit time (average time required for any given particle of tracer to pass through the tissue after an ideal bolus injection) can be estimated as

$$rCBV = \left(\int_0^{\infty} C_t(\tau) d\tau \right) / \left(\frac{\rho}{Kh} \int_0^{\infty} C_a(\tau) d\tau \right); rMTT = rCBV / rCBF. \quad (3)$$

Image sequences for in-vivo measurements were collected using 1.5T MRI scanner (SE-EPI with: 12 slices, 50 samples, TR=1.25-1.61s; TE=32-53ms; slice thickness 5-10 mm; 60 series - 3000 images). Using own, created software (Java) we extracted signals and concentration curves used in further processing to reconstruct rCBF, rCBV and rMTT parametric images. Three types of quantitative parametric images (CBF, CBV, MTT), synthesized under strictly controlled procedure, offer additional information for brain studies.

2. INFLUENCE OF DISPERSION AND DELAY

In quantitative DSC-MRI it is crucial to exactly measure an input, AIF function. Based on the AIF the required signal ($F * R(t)$) is deconvolved and used for quantitative maps synthesis. Theoretically the AIF describes concentration of contrast agent in the feeding vessel to the VOI. Practically it could be localized far away from VOI (carotid artery, middle cerebral artery). The path between measured AIF source and true AIF localization is unknown. The AIF delay and dispersion can be introduced using [2]:

$$C_a^{true}(t) = C_a(t) \otimes h(t) \quad (4)$$

where: $h(t)$ – vascular transport function, e.g.:

$$h(t) = \frac{1}{t_D} \cdot \exp\left(\frac{-t}{t_D}\right) \quad (5)$$

where: t_D - dispersion constant.

The influence of dispersion on final results (MTT or CBF) can be analyzed performing the following test. First the functions/signals of $C_a(t)$ and $R(t)$ are assumed

$$C_a(t) = \begin{cases} K(t-t_0)^\beta \cdot e^{-\alpha(t-t_0)}, & t > t_0 \\ 0, & t \leq t_0 \end{cases}, \quad (6)$$

$$R(t) = \exp\left(-\frac{t}{MTT}\right), \quad (7)$$

where: K , α , β model parameters (used $\beta=3$, $\alpha=2/3$), t_0 - bolus arrival time (BAT).

Then, the original $C_a(t)$ is convolved with the dispersion function for different values of the dispersion parameter t_D – equation (5). Finally, dispersed $C_a(t)$ functions are convolved with $R(t)$ producing a set of $C_t(t)$. Calculation of MTT/CBF requires to deconvolve the $R(t)$ from $C_t(t)$, assuming $C_a(t)$. Performing deconvolution of $R(t)$ for any $C_t(t)$ from the generated set, using the original (without dispersion) $C_a(t)$ can be used to analyze the influence of dispersion on MTT/CBF quality. Similar analysis may be used to analyze the influence of delay in $C_a(t)$ on final results. The delay in the test set can be introduced using shift of samples. Other steps are identical as for dispersion investigation.

Results

The influence of dispersion was estimated using 10 different values of t_D in the range of 0-7 seconds (typical MTT values for grey matter / white matter are 3-6s). Results (MTT as a function of t_D) are presented in Fig. 1b.

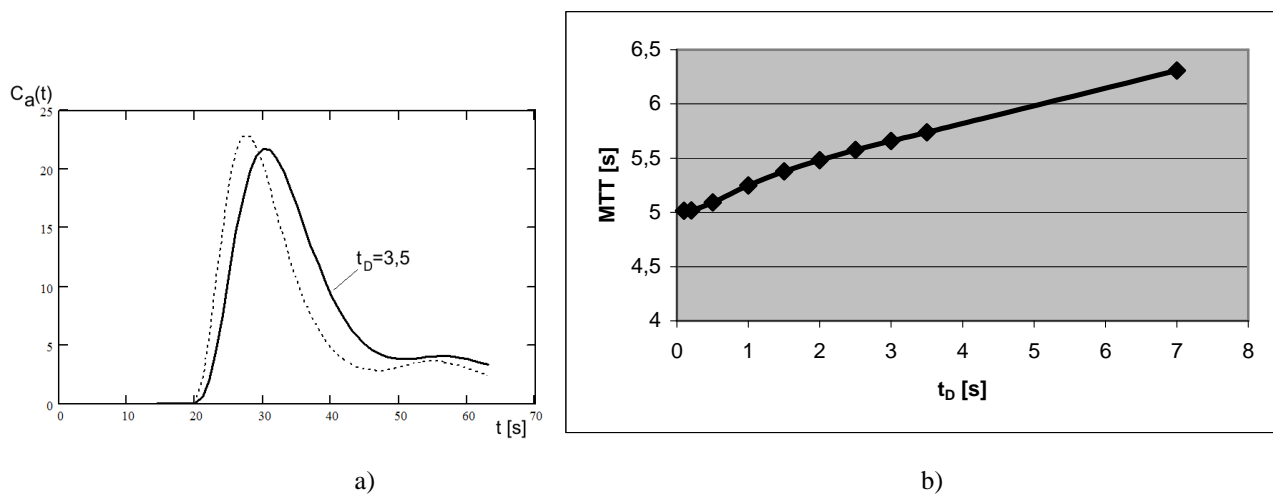


Fig.1. a) Example of the dispersion effect on $C_a(t)$. b) MTT as a function of dispersion (t_D) – true value of MTT=5

In the range of sampling period (in DSC-MRI usually 1-2s) the error caused by dispersion is 5-10%. This is a lower bound since for real signals (lower SNR) the influence of dispersion can be even higher.

Analysing the role of delay the shift in samples was used for the range -2 up to 5 samples (seconds). In Fig. 2a the results (MTT as a function of delay) of analysis are presented.

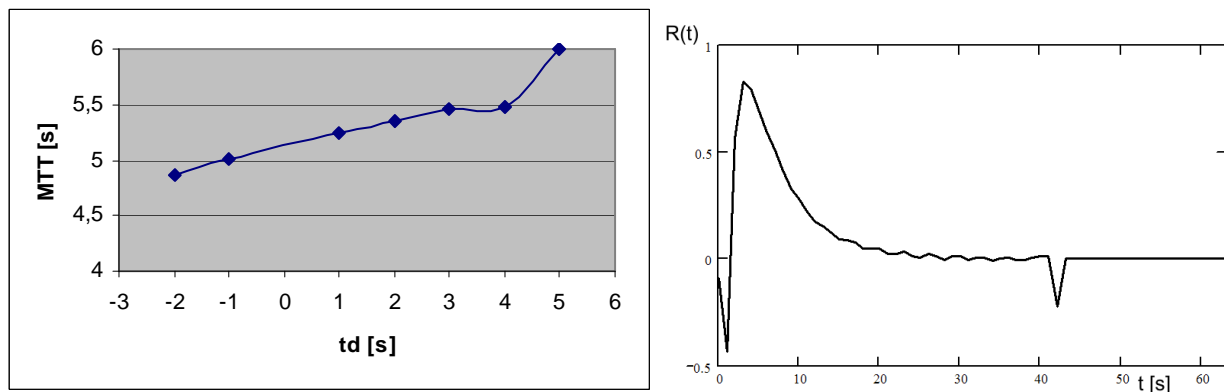


Fig.2. a) The influence of delay in $C_a(t)$ on MTT, true value of MTT=5s; b) deconvolved $R(t)$ for dispersed ($t_D=2$ s) and delayed (2s) $C_a(t)$

In the range of sampling period the error caused by delay is about 5%. In Fig. 2b the result of deconvolved $R(t)$ for dispersed ($t_D = 2s$) and delayed (2s) $C_d(t)$ is presented (compare to (7)). Unfortunately, the achieved result had required matrix regularization (ill-posed matrix, build with $C_i(t)$ for linear deconvolution). The TSVD method was used [6]. In the range of sampling period the error produced by both effect is up to 20%. However for real signals the dominated effect on errors can be related with SNR, and then with the regularization process.

3. INFLUENCE OF A SIGNAL NOISE

During a process of regularization it is very important to use appropriate regularization factor values, especially in a large disturbance of a signal. The experiments to analyze the influence of a signal noise and regularization factor values on perfusion parameters were investigated. Again the Gamma variate function was used with $K=1$, $\alpha=1$, $\beta=1$, $t_0=0$, to generate AIF (6). In the case of the $R(t)$ function (7), a value of the MTT parameter was fixed to 5 (seconds). Signal $C_i(t)$ was distorted by a noise described by a normal distribution with a mean value fixed to zero and following values of a standard deviation [0, 0.01, 0.05, 0.1, 0.3, 0.5, 0.7, 1]. Additionally, to avoid dependency on fixed parameters K , α , β , t_0 , F and MTT , a scale coefficient (maximum of $C_i(t)$) was used, which was multiplied by a standard deviation value. Tests were repeated 100 times to obtain mean results. Quantitative comparison between true and calculated parameter values were described using:

$$RMSE\% = \frac{1}{p} \sqrt{\frac{\sum_{i=1}^N (p_i - p)^2}{N-1}}, \quad Bias\% = \frac{1}{p} \sum_{i=1}^N \frac{(p_i - p)}{N} \quad (8)$$

where value p is a true value of a parameter, p_i is an estimated value of a parameter in every step i , where N - number of steps.

The goal of the tests was to obtain $RMSE$ and $Bias$ values as the function of introduced error (standard deviation), for CBF and CBV parameters.

In the first case a constant value of regularization coefficient was used ($= 10^{-2}$) (*Test 1*).

Next the optimal value of a regularization factor was automatically calculated. It was performed for two configurations: *Test 2* - optimization for CBF , *Test 3* - optimization for CBV . In the searching for the best values the assumed $R(t)$ function values (an initial guess) were used. In real those values are unknown but performed tests are only to investigate the role of a noise and regularization process.

Results

In Tab. 1 - Tab. 3 the example results for Test 1-3 are presented.

Tab. 1. Test 1 results: Fixed regularization value $\lambda = 10^{-2}$

δ	RMSE [%] - CBF	RMSE [%] - CBV	Bias [%] - CBF	Bias [%] - CBV
0	0	0	-0.7473	0.7511
0.01	12.4	14.4	0.0572	0.3788
0.05	66.7	75	2.6068	3.1749
0.1	121.7	143.3	7.3263	8.067
0.3	368.2	430	21.2142	23.5769
0.5	647.8	735	39.1494	43.3167

0.7	865.9	996.3	49.7286	55.8438
1	1189.5	1374.4	77.3399	84.2707

Tab. 2. Test 2 results: Optimization for a CBF

δ	RMSE [%] – CBF	RMSE [%] – CBV	Bias [%] - CBF	Bias [%] – CBV	λ
0	0	0.7511	-0.0164	-0.7473	0.01
0.01	0.0165	1.117	-0.0003	-1.0897	0.281
0.05	0.091	0.7639	-0.006	-0.4103	0.6355
0.1	0.1	1.4705	-0.0077	0.9641	0.8959
0.3	0.0994	6.1568	-0.0008	5.5812	1.6101
0.5	0.0901	10.955	0.0015	10.3718	2.0864
0.7	0.0832	15.6977	0.0005	14.8939	2.4954
1	0.0899	20.3769	0.0091	19.4394	2.985

Tab. 3. Test 3 results: Optimization for a CBV

δ	RMSE [%] – CBF	RMSE [%] – CBV	Bias [%] - CBF	Bias [%] – CBV	λ
0	0.0165	0.7511	-0.0164	-0.7473	0.01
0.01	12.7627	0.2306	11.333	-0.133	0.0397
0.05	4.3126	0.0204	2.5405	-0.0021	0.5832
0.1	17.0457	0.0276	-1.625	0	0.9932
0.3	13.0668	0.0419	-12.1171	0.0007	2.0242
0.5	18.3853	0.0481	-17.6852	0.0005	2.6869
0.7	22.2841	0.0555	-21.5229	0.0043	3.2307
1	24.8288	0.0567	-24.1608	0.0121	3.947

Using the fixed value of regularization factor the introduced noise has a large influence on the results. *RMSE* coefficient reached maximum of 1400% for the *CBV* parameter (similarly, *CBF* is near 1200%). In the *Bias* case, situation is similar. The obtained values are lower, maximum 85%, but sufficiently large to eliminate them from further analysis.

Analyzing results for the best case of the regularization factor there is not possible to set a one, universal value that guarantee the best accuracy of searching parameters. Optimal calculation of *CBV* (or *MTT*) and *CBF* requires to repeat deconvolution process. Analyzing regularization data, we see that along with increasing of the noise standard deviation, the regularization factor value also is raising. However it seems that the influence of the noise (in analyzed range) is not a critical factor in comparison to dispersion problems described earlier. Since the image sequence *SNR* can be controlled the more attention should be focused on appropriate *AIF* indication.

4. FINAL CONCLUSION

Performing appropriate quality assurance of measured signals and *AIF* extraction it is possible to reliable describe perfusion parameters using *DSC-MRI*. Since the method assumes the typical contrast-based procedure it can be easily used with most of current *MRI* scanners. The prepared software (Java) enables quantitative calculation of perfusion parameters for *DSC-MRI*. In Fig. 3 an example of graphical user interface with *EPI T2* image (first in the sequence measured during bolus tracking) and calculated *rBAT*, *rCBV* and *rCBF* images for a stroke case (limited perfusion in the observed left upper region) are presented.

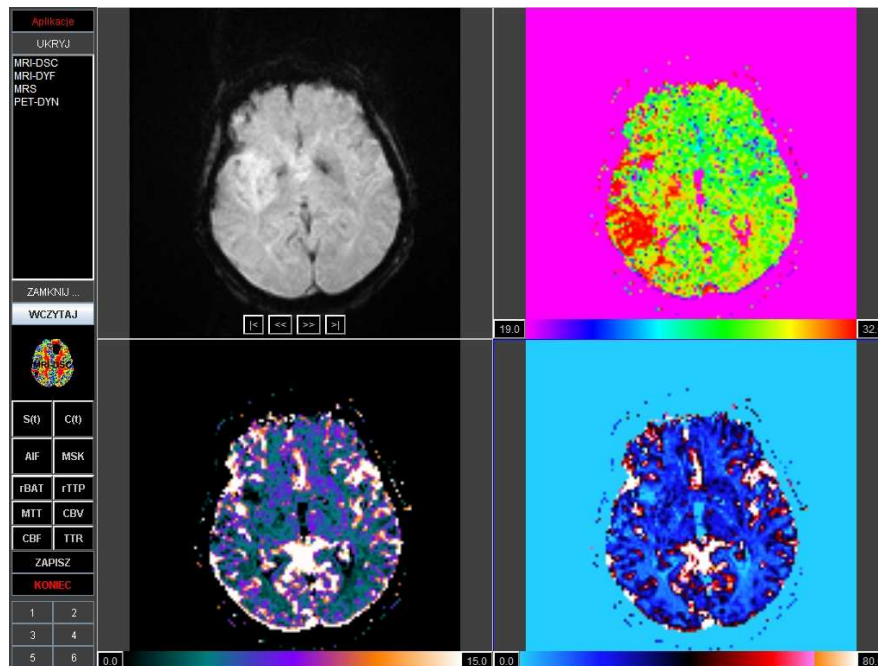


Fig. 3. An example of the graphical user interface with a set of images (from top left): EPI T2 and calculated rBAT [s], rCBV [ml/100g] i rCBF [ml/100g/min] for a stroke case

ACKNOWLEDGEMENT

This work was partly supported by the grant of Polish State Committee for Scientific Research (2003-2006) 4 T11E 042 25.

BIBLIOGRAPHY

- [1] CAI W., FENG D. D., FULTON R., Content based retrieval of dynamic PET functional images, *IEEE Transactions on Information Technology in Biomedicine* 4 (2)152-158, 2000.
- [2] CALAMANTE F, Gadian D G and Connelly A 2000 Delay and dispersion effects in dynamic susceptibility contrast MRI: simulations using singular value decomposition *Magn. Reson. Med.* **44** 466–73
- [3] ØSTERGAARD L, Weisskoff R M, Chesler D A, Gyldensted C and Rosen B R High resolution measurement of cerebral blood flow using intravascular tracer bolus passages: I. Mathematical approach and statistical analysis, II. Experimental comparison and preliminary results *Magn. Reson. Med.* **36** 715–36, 1996.
- [4] RUMINSKI J., KACZMAREK M., NOWAKOWSKI A., Medical Active Thermography – A New Image Reconstruction Method, LNCS2124, Springer, 274-281, 2001.
- [5] WANG J., ALSOP D. C., LI L., LISTERUD J., GONZALEZ-AT J. B., SCHNALL M. D., DETRE J. A., Comparison of Quantitative Perfusion Imaging Using Arterial Spin Labeling at 1.5 and 4.0 Tesla, *MRM* 48:242–254, 2002.
- [6] WU L., A Parameter Choice Method For Tikhonov Regularization, *Electronic Transactions on Numerical Analysis*. Volume 16, pp. 107-128, Kent State University, 2003.